Power and Phase of Alpha Oscillations Reveal an Interaction between Spatial and Temporal Visual Attention

Sayeed A. D. Kizuk and Kyle E. Mathewson

Abstract

■ Oscillatory brain rhythms can bias attention via phase and amplitude changes, which modulate sensory activity, biasing information to be processed or ignored. Alpha band (7–14 Hz) oscillations lateralize with spatial attention and rhythmically inhibit visual activity and awareness through pulses of inhibition. Here we show that human observers' awareness of spatially unattended targets is dependent on both alpha power and alpha phase at target onset. Following a predictive directional cue, alpha oscillations were entrained bilaterally using repetitive visual stimuli. Subsequently, we presented either spatially cued or uncued targets at SOAs either validly or invalidly predicted in time by the entrainers. Temporal validity maximally modulated perceptual performance outside the spatial focus of attention and was associated with both increased alpha power and increased neural entrainment of phase in the hemisphere processing spatially unattended information. The results demonstrate that alpha oscillations represent a pulsating inhibition, which impedes visual processing for unattended space. ■

INTRODUCTION

Sensation requires boosting activity representing stimuli occurring at certain locations and times at the expense of others (Posner, 1980). When attention is cued to particular locations in space, RT, detection, and discrimination improve (Posner, 1980), and evoked neural activity is increased (Müller, Teder-Sälejärvi, & Hillyard, 1998). Alpha oscillations (7–14 Hz) are one mechanism by which spatial attention biases sensory activity (Jensen, Gips, Bergmann, & Bonnefond, 2014; Mathewson et al., 2011; Jensen & Mazaheri, 2010; Klimesch, Sauseng, & Hanslmayr, 2007). Alpha power decreases following cues in brain areas representing attended regions of space (Kelly, Lalor, Reilly, & Foxe, 2006; Thut, Nietzel, Brandt, & Pascual-Leone, 2006), increasing evoked activity (Romei, Brodbeck, et al., 2008; Romei, Rihs, Brodbeck, & Thut, 2008), and improving performance (Mathewson, Gratton, Fabiani, Beck, & Ro, 2009; Ergenoglu et al., 2004).

Cueing participants to upcoming moments enhances performance and increases neural activity, a form of temporal attention involving top–down control (Buhusi & Meck, 2005; Coull & Nobre, 1998). Decreased alpha power during periods of expected target appearance also increases evoked activity and improves performance (Rohenkohl & Nobre, 2011; Min et al., 2008). This top–down attention differs from bottom–up temporal expectancies, which automatically induce enhanced detection and evoked neural activity in-time with rhythmic external stimuli (Breska & Deouell, 2014; Large & Jones, 1999). This bottom–up temporal attention, occurring at shorter timescales (<1 sec), involves phase-locking oscillatory activity to rhythmic stimulation (Schroeder & Lakatos, 2009).

Cellular firing and gamma oscillations are boosted during particular phases of local field potentials (Bonnefond & Jensen, 2015; Spaak, Bonnefond, Maier, Leopold, & Jensen, 2012; Haegens, Nácher, Luna, Romo, & Jensen, 2011; Lőrincz, Kékesi, Juhász, Crunelli, & Hughes, 2009; Jacobs, Kahana, Ekstrom, & Fried, 2007). Ongoing oscillatory phase in the EEG cyclically modulates evoked activity (Sheeringa et al., 2011; Mathewson et al., 2009; Barry et al., 2004; Jansen & Brandt, 1991), and alpha phase specifically modulates RT (Drews & VanRullen, 2011; Hamm, Dyckman, Ethridge, McDowell, & Clementz, 2010; Callaway & Yeager, 1960) and perception (Cravo et al., 2015; Hanslmayr, Volberg, Wimber, Dalal, & Greenlee, 2013; Dugué, Marque, & VanRullen, 2011; Busch & VanRullen, 2010; Busch, Dubois, & VanRullen, 2009; Mathewson et al., 2009; Varela, Toro, John, & Schwartz, 1981).

Exogenous rhythmic stimuli also cyclically modulate behavioral performance (Hickok, Farahbod, & Saberi, in press; Lawrance, Harper, Cooke, & Schnupp, 2014; Rohenkohl, Cravo, Wyart, & Nobre, 2012; Mathewson, Fabiani, Gratton, Beck, & Lleras, 2010; Jones, Moynihan, MacKenzie, & Puente, 2002) by locking a "preferred" oscillatory phase to the timing of rhythmic entrainers (ten Oever, van Atteveldt, & Sack, 2015; Gray, Frey, Wilson, & Foxe, 2015; Henry, Herrmann, & Obleser, 2014; Spaak, de Lange, & Jensen, 2014; Cravo et al., 2012; Henry & Obleser, 2012; Besle et al., 2011; Stefanics et al., 2010). This induced phase locking provides a mechanism for

University of Alberta

doi:10.1162/jocn_a_01058

bottom–up temporal expectancies' influence on brain activity and behavior. These exogenous neural and perceptual entrainment effects are, like endogenous effects of phase on perception, maximal for rhythms in the alpha band (de Graaf et al., 2013; Pastor, Artieda, Arbizu, Valencia, & Masdeu, 2003; Herrmann, 2001).

We predict that spatial and temporal attention can therefore be instantiated by alpha power and phase, respectively. We have proposed a mechanistic theory of alpha oscillations as a pulsating inhibition, where periods of high alpha power involve larger and longer periods of neural inhibition associated with particular oscillatory phases (Mathewson et al., 2009, 2011). We therefore predict that spatial and temporal attention should interact, and this interaction should be mediated in the brain by alpha power and phase. Rhythmic stimuli should better entrain the phase of alpha oscillations where they are larger in amplitude ipsilateral to the direction of attention and more effectively cyclically bias visual activity and behavior.

To test this proposed interaction between power-mediated spatial attention and phase-mediated temporal expectancy, targets were spatially cued either validly or invalidly and presented either in-time or out-of-time with preceding, bilateral 12-Hz rhythmic entrainers (Mathewson et al., 2010, 2012). An interaction between temporal and spatial attention is predicted, such that the expected benefit for temporally predictable targets will be enhanced outside the focus of spatial attention, where overall performance should be worse. Concurrent findings of an interplay between alpha power and phase locking would imply their complementary and interactive roles in spatial attention and temporal expectancies.

METHODS

Participants

A total of 43 paid volunteers (age = 19.089–36.025 years, M = 23.058, SD = 3.238; 27 women; 7 left-handed) from the University of Alberta community gave informed consent, as approved by the internal research ethics board. All participants reported normal or corrected vision and were compensated with a $10 honorarium for their participation. Data from one participant were removed because of noncompletion of the experiment. Additional preplanned screening of participants based on behavior is described below.

Materials and Procedure

A bilateral, directionally cued metacontrast masking paradigm (Boyer & Ro, 2007) with preceding entrainment (Mathewson et al., 2010, 2012) was used to test for interactions between spatial and temporal attention. Figure 1 shows the stimulus dimensions (A) and the timeline for a representative trial (B).

On each trial, participants were instructed to fixate the black central cross, presented continuously during the entire block. After a pretrial period of 400 msec, a black isosceles triangle directional cue was presented above fixation, centered on the vertical meridian, for 200 msec. Participants were instructed to remain fixated on the central cross and attend covertly to the side cued. Spatial cues were 70% predictive of the target location. The cue was followed by a postcue period showing only the fixation cross for 1000 msec. Subsequently eight entrainment annuli (30.47% gray) were presented bilaterally for 8.33 msec (one refresh) with seven blank ISIs between annuli of 75 msec. The SOA for the annuli was thus 83.3 msec, constituting a 12-Hz rhythmic presentation.

After the onset of the final entrainer, one of four short SOAs was pseudorandomly chosen (with equal number of trials of each condition in each block) to be used as the SOA between the final pretarget entrainer and the target. Two SOAs were in-time with the rhythmic entrainers (83.3 and 166.6 msec), and two SOAs were out-of-time with the entrainers (41.6 and 124 msec). After this lag, a unilateral circular target (8.33 msec) was pseudorandomly chosen to appear either on the left or right side, validly cued by the directional cue 70% of the time. The targets outside edge met the inside edge of the flashing entrainers and mask but did not spatially overlap. The target luminance was adjusted for each participant based on a staircasing procedure described below. The 8.33-msec backward mask appeared bilaterally following the target on every trial after a 50-msec ISI chosen to maximize masking (Boyer & Ro, 2007). The mask was identical to the annulus entrainers. The entrainment annuli, target, and mask were presented entirely above the horizontal meridian, so that stimuli always appeared in the upper visual field, situated such that the bottom edge of the annuli touched the horizontal meridian.

Following the mask offset, participants responded to the target location using left and right arrow keys with their left and right index fingers, respectively. If they did not detect a target at either location, they were instructed to guess. The next trial began 500 msec after their response. The validity of the cue direction and the target timing after the preceding entrainers created four conditions—spatially valid in-time, spatially valid out-of-time, spatially invalid in-time, and spatially invalid out-of-time. Participants completed 12 blocks of 48 trials (12 trials of each SOA), completing an average of 82.89 trials per each SOA in the valid condition (M = 83.59, 82.91, 80.86, 84.14; SD = 5.93, 3.68, 5.78, 6.31) and 34.13 trials per SOA in the invalid condition (M = 32.73, 33.95, 35.27, 34.55; SD = 5.26, 4.02, 5.75, 5.46). On 20% of the trials the target and mask did not appear to measure the state of the brain at the moment of target onset without contamination from target-evoked potentials. Participants were given extensive instructions and example trials of each type in slow motion and real time prior

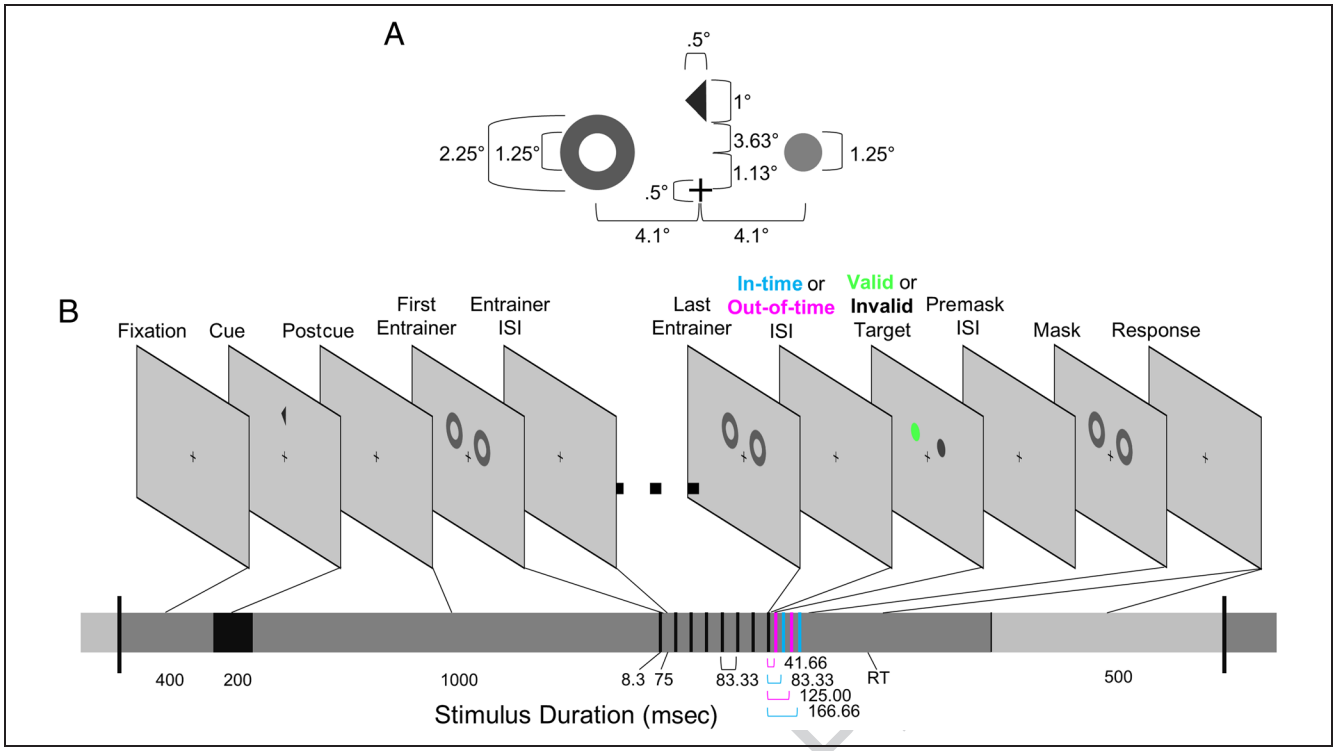

Figure 1. Spatiotemporal attention task stimulus dimensions and trial timeline. (A) Stimuli (size in visual degrees; not shown to scale) were presented on a 50% gray background to participants sitting 57 cm from a 120-Hz rastering LCD monitor. (B) Schematic showing representative trial in which participants fixate a central cross and are cued to attend (left or right) to one of two upcoming target locations. After a fixed delay, a series of synchronous bilateral annuli are presented around the upcoming target locations, at a fixed rate of 12 Hz. Following the final entrainer, a circular target was presented at either the spatially valid (green) or invalid location (black; 70% validly cued; 20% catch trials) at one of four random delays: two in-time with the preceding rhythmic annuli (blue) and two out-of-time (magenta; 50% in-time). The target was then masked with a bilateral annulus mask at a fixed delay making target detection difficult. Participants then indicated the side (left or right) that the circular target appeared before beginning the next trial. Target luminance was adjusted for each participant prior to the experiment in a staircasing procedure to 60% detection performance in an estimated psychometric function for spatially valid targets in-time with the preceding entrainers.

to the experiment. Participants were allowed to rest at their own pace between blocks.

Participants sat in a dimly lit and soundproof chamber, 57 cm from a 1920 × 1090 pixel^2 (22.5 in. diagonal) ViewPixx/EEG LCD monitor (VPixx Technologies) with a refresh rate of 120 Hz, simulating a CRT display with LED backlight rastering. The rastering along with 8-bit digital TTL output triggers yoked to the onset and value of the top left pixel allowed for submillisecond accuracy in pixel illumination times, which were confirmed with a photocell prior to the experiment. Stimuli were presented on a 50% gray background with a Windows 7 PC running Matlab R2012b with the Psychophysics toolbox (Version 3; Brainard, 1997). Video output was sent to the ViewPixx/EEG with an Asus Striker GTX760 graphics processing unit.

Individual Detection Threshold

Individual detection threshold for spatially valid, in-time targets was estimated for each participant prior to starting the task using the Quest staircasing procedure in Psychtoolbox (Watson & Pelli, 1983). Participants performed a modified version of the task where they only responded to whether or not they detected the spatially valid, in-time target, using their left and right index fingers to answer detected or undetected with the up or down arrows. On the first trial of each block, the target was set to the background gray so that it was undetectable. Subsequent undetected responses darkened the target stimulus, whereas detected responses lightened the stimulus. After four blocks of 30 staircasing trials were completed (beta = 3.5; delta = .01; gamma = 0), the final threshold estimates were averaged across the four blocks and used to estimate a 60% detection rate threshold for use in the main portion of the experiment. After the main task, data from participants that still showed more than 90% detection rate in the spatially invalid condition during the experimental trials were also not considered to ensure that the effect of spatial validity would be detectable in all participants and to avoid any ceiling effects. As a result, behavioral and electrophysiological data from 18 participants were not considered at all in the analyses ($M_{invalid}$ = .945, SD = .032). This left 24 participants (age 19.464–26.917, M = 22.211, SD = 1.863; 17 women; 3 left-handed) to be included in the analyses ($M_{invalid}$ = .714, SD = .135). Note that participants could guess with 70% accuracy by reporting the

cued location. However, this would lead to 100% correct detection for the cued location and 0% detection for the uncued location, and we did not see this pattern either in the grand average or the individual level.

Behavioral Analysis

For each participant, we computed the left/right discrimination accuracy for targets at each of the four SOAs following the final entrainer, separately for spatially valid and invalid targets. We computed the main effect of spatial attention as the difference in the proportion of correct answers collapsed across the four SOAs. We computed the main effect of temporal attention as the difference in the proportion of correct answers collapsed across spatial validity, combining the two in-time and out-of-time SOAs. We also combined the two in-time and two out-of-time SOAs for the interaction. To avoid early responses and distracted trials, we only considered trials with RTs greater than 200 msec and less than 2 sec, removing an average of 3.614 trials (SD = 4.276) per participant.

EEG Recording

EEG was recorded from 15 scalp locations (O1, O2, P7, P3, Pz, P4, P8, T7, C3, Cz, C4, T8, F3, Fz, F4; 10/20 system) and the right mastoid, referenced online to an electrode affixed to the left mastoid, with a ground channel at Fpz, using 18 Ag/AgCl sintered ring electrodes (EasyCap) in a 20-channel electrode cap (EasyCap), and amplified with a 16-channel V-amp amplifier (Brain Products, München, Germany). The impedance between skin and electrode was reduced using abrasive tape and Abralyt gel until impedance from every electrode was below 10 kΩ. Electrode locations were re-referenced offline to the average of the left and right mastoids. The bipolar vertical and horizontal EOG was recorded with additional electrodes using two BIP2AUX converters in the V-amp auxiliary channels (Brain Products). Electrodes were placed 1 cm lateral from the outer canthus of each eye and above and below the left eye. These EOG electrodes had their own ground affixed in the central forehead.

Data were recorded at 1000 Hz with a resolution of 24 bits (0.049 μV steps). Online filters of 0.629-Hz high-pass and 200-Hz lowpass were used. Data were collected inside a sound and radio frequency-attenuated chamber (40A-series; Electro-Medical Instruments, Mississauga, Ontario, Canada), with copper mesh covering a window. The lights were left on, and the window was covered during experiments. The only electrical devices inside the chamber were the amplifier, powered from a battery-powered laptop located outside the chamber, speakers, keyboard, and mouse, all powered from outside the room, the ViewPixx monitor, powered with DC power from outside the chamber, and a battery-powered intercom. Nothing was plugged into the internal power outlets, and any electrical devices (e.g., cell phones) were removed from the chamber during recording.

EEG Preprocessing

All analyses were completed using Matlab R2012b with the EEGLAB (Delorme & Makeig, 2004) and CircStat (Berens, 2009) toolboxes, as well as custom scripts. For cue-locked power and phase-locking analysis, trials were divided into 5500-msec segments locked to the onset of the spatial attentional cue, including a 1500-msec baseline period precue. The average voltage in the 200 msec of this baseline prior to the cue was subtracted on each trial for every electrode. Trials with absolute voltage fluctuations on any channel greater than 1000 μV were discarded. Eye movements were then corrected with a regression-based procedure developed by Gratton, Coles, and Donchin (1983). After identifying blinks with a template-based approach, this technique computes propagation factors as regression coefficients predicting the vertical and horizontal eye channel data from the signals at each electrode. The eye channel data are then subtracted from each channel, weighted by these propagation factors, removing any variance in the EEG predicted by eye movements. The uncorrected horizontal eye channel also allowed us to test for any systematic eye movements following left versus right cues. We found no systematic differences between left and right cue conditions, except one participant whose eye movements indicated that they were following the directional cue overtly. Data from this participant were not included in any analyses. Finally, after a second baseline subtraction with the 200 msec precue, trials with remaining absolute voltage fluctuations on any channel greater than 500 μV were removed from further analysis. Data from one participant were extremely noisy resulting in many rejected trials, and their data were also therefore not included in the analysis. In total, this left 22 remaining participants on which all behavioral and electrophysiological analyses are computed (age 19.464–26.917, M = 22.215, SD = 1.944; 16 women; 3 left-handed), with an average of 555.73 (SD = 49.14) of their original 576 trials remaining for analysis after artifact rejection.

Lateralized Alpha Oscillations

To estimate the cue and entrainer locked oscillatory activity, a time–frequency analysis of the preprocessed data was performed using the newtimef() function in the EEGLAB toolbox (Delorme & Makeig, 2004) on the data from −1500 precue to 3500 msec postcue. A moving window fast Fourier transform (FFT) estimated power and phase for 81 linear-spaced frequencies between 1 and 40 Hz, with a Hanning window length of 512 time points (512 msec) and no baseline period subtraction. For all analyses of power, we first log-transformed the

values derived from the FFT to normalize power values and minimize the influence of extreme values on lateralization index and statistical tests. We confirmed the effectiveness of this technique (data not shown) by normalizing the single trial measures of lateralized alpha power.

To examine the preparatory lateralization of alpha oscillations following the cue, we compared the log-transformed power over time in the alpha band between the frequencies of 7 and 14 Hz, a broad range intended to cover the full range of intersubject variability in peak alpha frequency (data not shown; Haegens, Cousijn, Wallis, Harrison, & Nobre, 2014), comparing electrodes ipsilateral versus contralateral to the direction of the cue. We computed the average log-transformed alpha power for the electrode ipsilateral to the cue on both left and right cued trials and subtracted the average log-transformed alpha power for the electrode contralateral to the cue on both left and right cued trials. We computed the average ipsilateral and contralateral power in two separate windows: the latter half of the period between cue onset and entrainer onset (600–1200 msec) and during the target period between the last entrainer onset and the last possible target onset (1783–1950 msec). Note that we did not use a baseline correction in the frequency domain for our power analysis because all our measures consider the difference in power and phase locking between two electrodes.

Phase-locking Index

To estimate the efficacy of our annulus entrainers at locking the timing of oscillations in the brain, we considered the consistency of the 12-Hz phase across trials during and following the entrainment period. The phase consistency across the trial was measured using the ITC output from the newtimef() function, which uses the complex average phase across trials once the power on each trial is set to 1. This analysis was computed for both target-present and target-absent trials independently. For each participant, a phase-locking index (PLI) was computed as the average ITC value between 10 and 14 Hz, reflecting a narrowed frequency range centered around the 12-Hz rhythm at which the entrainers were presented, within the period between the onset of the first entrainer and the onset of the last entrainer (1200–1783 msec), as well as in the target period from the previous analysis. To test for interactions with spatial attention, electrodes ipsilateral and contralateral to cue direction were compared in a subsequent analysis.

Target-locked ERPs

To measure the peritarget entrained oscillatory activity as a function of temporal and spatial attention, we analyzed visual ERP components time-locked to the onset of targets and to the time of the missing target on target-absent trials. Segments of EEG data from −1000 before to 2000 msec after the target were baseline-subtracted with the average value in the 200 msec pretarget. Artifact rejection and correction procedures were used identical to those described above, except for the additional use of a 30-Hz low-pass FIR filter (eegfilt() in EEGlab). These data were computed at Pz for an overall analysis of temporal attention and at electrodes lateralized with respect to the direction of attention at P3 and P4 for an analysis of the interaction between temporal and spatial attention. Target-present and target-absent trials were considered separately.

12-Hz Phase at Target Onset

To estimate the relative phase at the onset of targets appearing either in-time or out-of-time with the preceding entrainers (Mathewson et al., 2009, 2012), with no influence from target- and mask-evoked activity, we measured single trial phase in only the 20% of trials in which no target or mask was presented, but time-locked to the moment targets would have occurred. Our presentation procedure still randomly assigned one of four SOAs after the final entrainer for the blank target, so we used these as independent trial groups to measure the instantaneous phase at the time targets would have occurred for both in-time and out-of-time targets. Segments of EEG data from −1000 before to 2000 msec after the missing target were baseline-subtracted by the average value in the 200 msec pretarget. Artifact rejection and correction procedures were used identical to those described above. Power and phase for 81 linear-spaced frequencies between 1 and 40 Hz were estimated with a moving window FFT on data from −1000 pretarget to 2000 msec posttarget with a window length of 512 time points (512 msec) and no frequency domain baseline period subtraction.

The phase values at electrode Pz for the 512-msec FFT window, centered at the missing target onset at a frequency of 12.207 Hz were considered (the frequency closest to the stimulation frequency). First, these phase values were divided into separate groups of independent trials for moments in-time and out-of-time with the rhythmic preceding entertainers. Circular mean phase for both in-time and out-of-time missing targets was also computed for each participant, as well as the radial difference between these circular means, and the grand mean of these radial differences across participants. We then tested the reliability of these differences with a Hotelling bivariate F test against a difference of zero degrees. Lastly, we tested whether the difference in phase between in-time and out-of-time targets was more divergent in the ipsilateral electrode compared with the contralateral electrode, using a Hotelling bivariate F test against a difference of zero degrees. Circular statistics were computed with custom scripts and the CircStat toolbox (Behrens, 2009; Zar, 1999; Fisher, 1993). To test for interactions

between this single-trial phase entrainment and spatial attention, we also computed each step of this analysis separately for electrodes P3 and P4 and sorted them based on the electrode locations ipsilateral versus contralateral to the direction of attention.

RESULTS

Behavioral Interactions between Spatial and Temporal Attention

Figure 2A shows the target detection for each lag between the last entrainer and target onset SOA (42, 83, 125, 167 msec), revealing a cyclical modulation in performance yoked to the preceding entrainers (Mathewson et al., 2010, 2012). Figure 2B shows the proportion of correctly detected targets collapsed into the two conditions of spatial validity (valid: the target appeared in the attended hemifield; invalid: the target appeared in the unattended hemifield) and target timing (in-time: the target was in-phase with the rhythmic entrainers; out-of-time: target was out-of-phase with the rhythmic entrainers). A 2 × 2 repeated-measures ANOVA revealed improved accuracy for spatially valid targets (M = 0.843, SD = 0.097) compared with spatially invalid targets (M = 0.710, SD = 0.141; main effect of spatial validity $F(1, 21) = 23.155$, $p = .00009$). Also as previously found in detection tasks (Mathewson et al., 2010, 2012), there was improved accuracy for targets in-time (M = 0.794, SD = 0.092) compared with targets out-of-time with the preceding entrainers ($M = 0.758$, $SD = 0.117$; main effect of temporal validity $F(1, 21) = 11.392$, $p = .0029$).

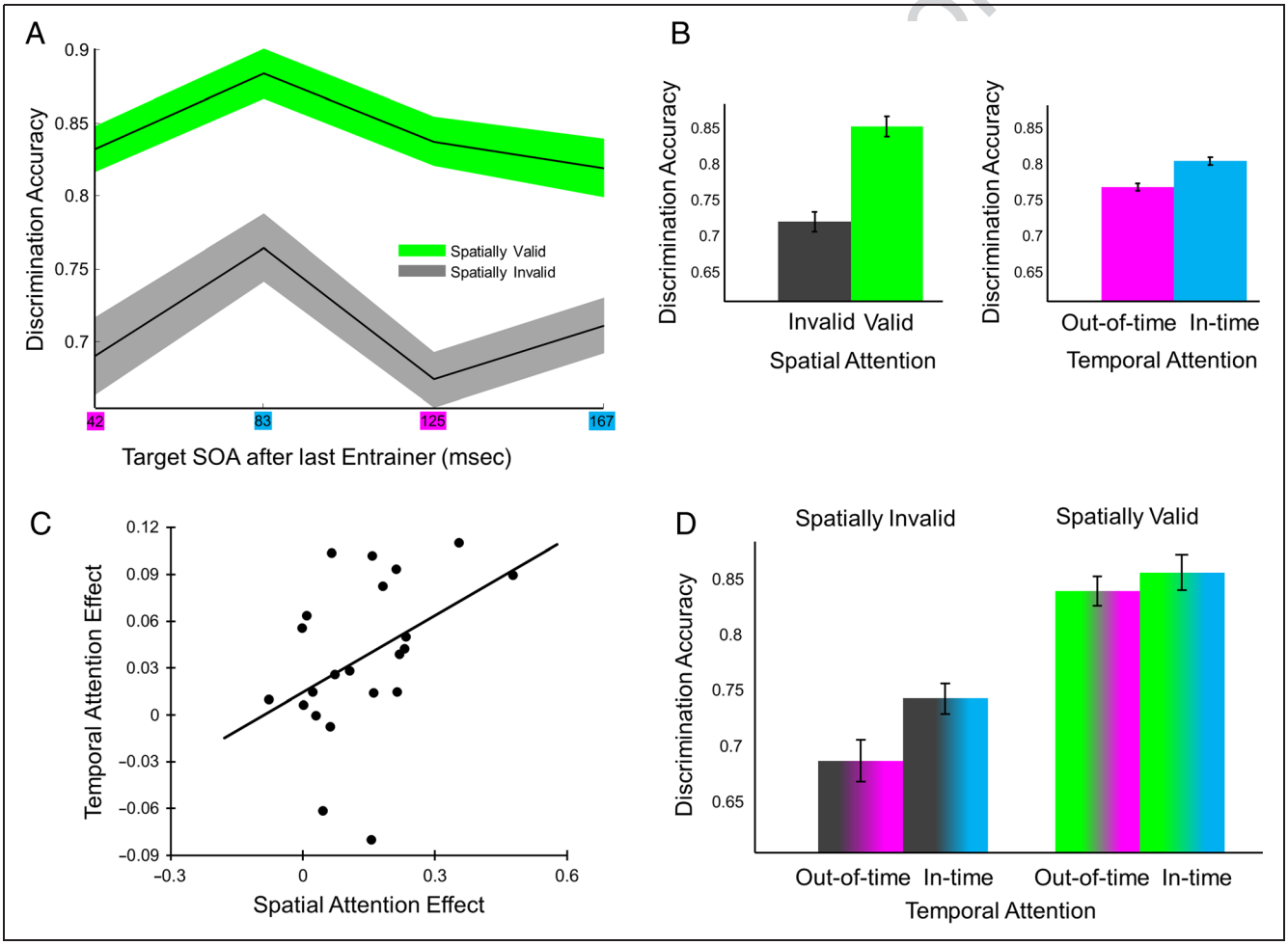

Figure 2. Spatial and temporal attention effects on discrimination and their interaction. (A) Target location discrimination performance as a function of spatial validity and target timing. Accuracy was better for spatially valid targets and for targets in-time with the entrainers. Shaded regions shows within-participant *SEM* (Loftus & Masson, 1994). (B) Main effects of spatial and temporal attention are shown by collapsing across conditions in A, showing greater accuracy for spatially valid (green) compared with invalid (black) targets, as well as for in-time (blue) versus out-of-time (magenta) targets. Error bars represent within-subject *SEM*. (C) A scatterplot of the spatial versus temporal attention effects (in-time–out-of-time) show that participants with larger spatially validity effects also had larger effects of temporal expectancy on behavioral accuracy. The normalized regression line is plotted, projected past the data for clarity. (D) Spatial and temporal attention interacts such that the accuracy improvement for in-time targets was larger in the spatially invalid location. The left side color of each bar indicates the spatial attention condition, the right side the temporal attention condition.

Figure 2C shows that these effects are correlated; participants with larger spatial cueing effects trended toward also having larger benefits for targets cued in time by rhythmic entrainers ($r = .421$, $t(20) = 2.077$, $p = .0508$), as would be expected if they relied on similar oscillatory mechanisms.

Figure 2D shows the novel interaction between the two types of attention. The interaction was such that the temporal attention effect was larger for targets at the spatially invalid location (in-time–out-of-time; $M = 0.056$, $SD = 0.084$) than at the spatially valid location ($M = .017$, $SD = 0.04$; spatiotemporal interaction $F(1, 21) = 4.476$, $p = .0465$). Two post hoc comparisons were also made to assess the effect of temporal validity within each spatial validity condition, using the Bonferroni method with a corrected alpha of .05/2 = .025. The tests revealed that, within the spatially invalid condition, there was a significant difference between in-time ($M = 0.74$, $SD = 0.12$) and out-of-time targets ($M = 0.68$, $SD = 0.17$; $t(21) = -3.10$, $p = .003$). When the target was spatially valid, the difference in detection between targets in-time ($M = 0.85$, $SD = 0.10$) and out-of-time with entrainers ($M = 0.83$, $SD = 0.10$) was not reliable when correcting for multiple comparisons ($t(21) = -1.84$, $p = .040$), confirming that the effect of temporal attention was only statistically significant for spatially invalid trials.

It is possible that our participants were biased to respond more to the cued or uncued location when unsure about the target location. An analysis of the 20% of trials where no target was present however revealed no preference for either side ($M_{cued} = 0.5486$, $SEM = 0.0298$, $t(21) = -1.63$, $p = .1178$). This lack of a significant preference for either the cued or uncued side when no information was present about target location indicates that participants were not using any strategy based on the cue validity but were in fact attempting to discriminate between the two choices, as we had intended.

Spatial Attention Lateralizes Alpha Power

We next sought to examine the degree of 7–14 Hz lateralization associated with spatial attention throughout the trial. Figure 3A shows the lateralized alpha power from electrodes P3 and P4, plotted as the log-transformed power at the electrode ipsilateral to the cued direction of attention minus the log-transformed power at the electrode contralateral to the cued direction. Two windows were identified as being most appropriate to examine lateralized alpha effects, a cue window (600–1200 msec postcue) leading up to the start of the entrainment period, and a target window (1783–1950 msec), which reflects the period from the onset of the last entrainer until the onset of the last target presentation. During this target period, participants would be attending the cued location for the target. Scalp topographies averaging over the frequencies of 7–14 Hz for both the cue and target windows show a central-parietal distribution. Figure 3B shows increased alpha power observed in the electrode ipsilateral to the cued direction ($M_{early} = 0.153$, $SD_{early} = 0.365$; $M_{late} = 0.062$, $SD_{late} = 0.341$) compared with the electrode contralateral to the cued direction of attention in both the cue ($M = 0.142$, $SD = 0.370$; $t(21) = 3.436$, directional $p = .0012$) and target time windows ($M = 0.053$, $SD = 0.341$, $t(21) = 2.039$, directional $p = .0271$), demonstrating the expected lateralization of alpha power away from the direction of attention. Figure 3C shows as expected that participants with more lateralized alpha with respect to the direction of attention also showed a greater benefit of spatial cue validity, although this trend did not reach significance ($r = .241$, $t(20) = 1.109$, one-tailed $p = .140$).

Entrainers Phase-lock Ongoing Neural Activity that Predicts Temporal Attention

To test for the main effects of target timing irrespective of spatial attention, we measured phase-locking from a central electrode first, replicating past work with similar tasks (Mathewson et al., 2012). Figure 4A shows the PLI at electrode Pz averaged over spatial cue direction for target-present trials, and Figure 4B shows the same for target-absent trials. In addition to broadband increases in apparent phase locking because of time-locked stimulus-evoked activity, a sustained and clear increase in PLI is observed to be centered at the 12-Hz entrainment frequency, which begins at the start of the entrainment period and continues through the target period (Mathewson et al., 2012). Scalp topographies were computed by averaging across the frequencies between 10 and 14 Hz within these time windows and show a strong posterior-central distribution for the entrained activity. Figure 4 (C and D) plots for target-absent trials the peristimulus time of the broadband ERP locked to the missing target onset for both out-of-time and in-time targets, showing the 180° difference in the phase of dominant alpha oscillations. Spatially valid and invalid labeled trials in Figure 4C indicate separate groups of trials, confirming the robustness of this effect.

To quantify this difference in phase, we next compared the phase of the entrained 12-Hz oscillation at target onset between in-time and out-of-time targets, using only the trials in which no target was actually present to avoid the influence of evoked activity (Samaha, Bauer, Cimaroli, & Postle, 2015; van Diepen, Cohen, Denys, & Mazaheri, 2015). It was expected that moments in-time versus out-of-time with the entrainers would show a separation of 180° in the average 12-Hz phase. Figure 4E shows histograms of these single-trial phases pooled over all trials and participants, revealing nonuniform and opposite distributions in 12-Hz phase at targets in-time ($M = 296.398°$) and out-of-time ($M = 121.984°$) with the preceding rhythm.

To confirm this difference in phase, we also computed for each participant the circular mean of the 12-Hz phase at

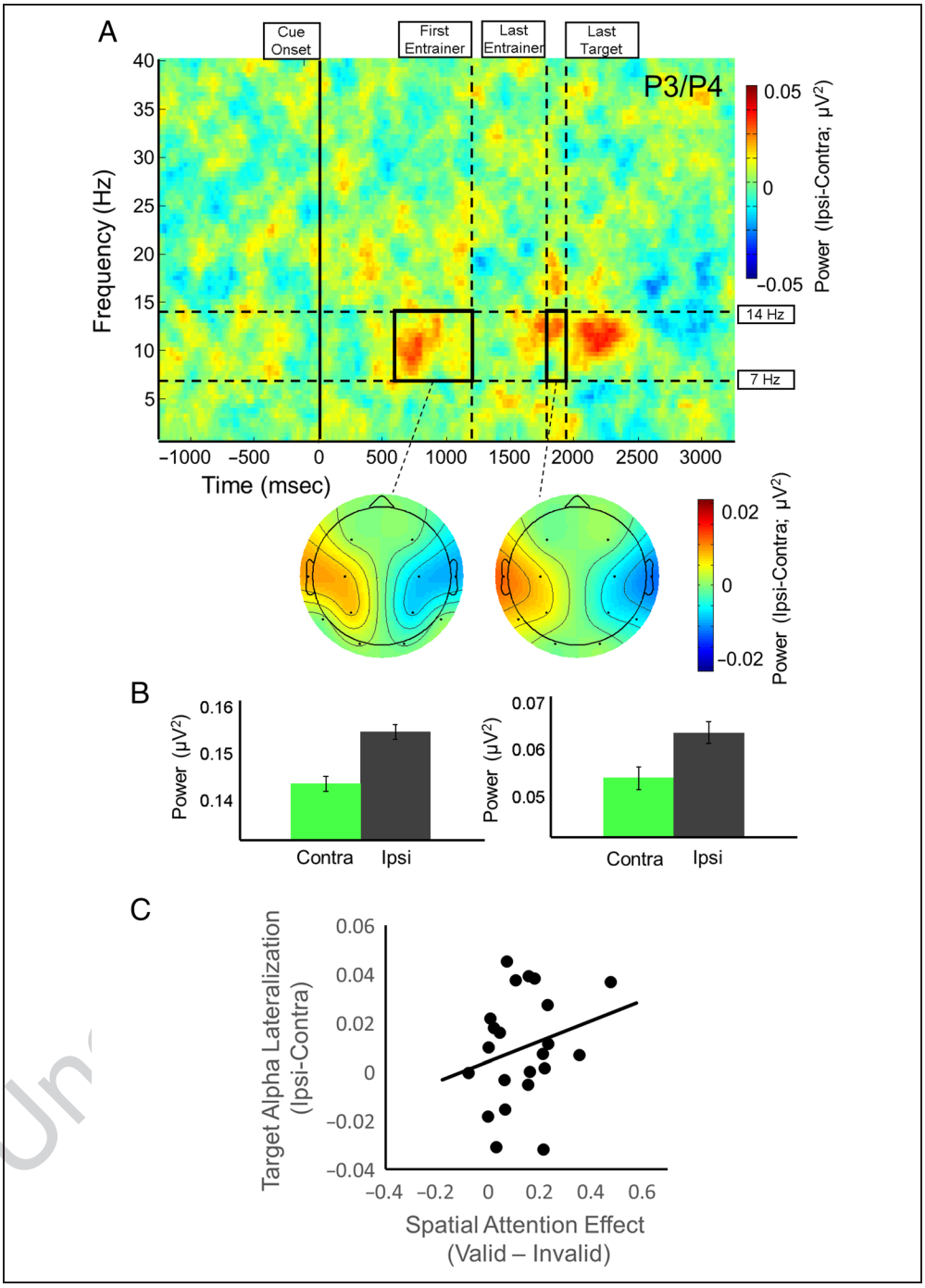

Figure 3. Spatial attention lateralizes alpha oscillations and improves performance. (A) A lateralized time–frequency spectrogram of the oscillatory power computed with a moving window FFT subtracting electrodes (P3 or P4) contralateral to the spatial attention cue from those ipsilateral. Red regions show more lateralized alpha power following the cue onset, during the entrainer period, and extending into the target period. Scalp maps are depicted averaged over the alpha band (7–14 Hz), in early (postcue) and late (target period) time windows, and computed by subtracting contralateral from ipsilateral bilateral electrodes and plotting them on the left hemisphere while switching the signs for the right hemisphere (simulating a leftward shift of attention). (B) Alpha power was lateralized with attention such that there was lower power contralateral (green) compared with ipsilateral (black) from the direction of cued spatial attention, both in the postcue and target time periods. Error bars represent within-participant *SEM*. (C) Participants who lateralized their alpha oscillations with attention more during the target period (ipsilateral vs. contralateral with attention) trended toward showing increased performance benefits from spatial attention (valid–invalid accuracy).

target onset, separately for targets in-time (M = 299.207°) and out-of-time with the entrainers (M = 120.460°). Figure 4F shows for each participant the radial difference in phase between targets in-time and out-of-time. The relative sign is kept intact to allow the values to range around the full circle, revealing a reliable difference in phase around 180° (M = 183.579°; Hotelling's bivariate $F(1, 20)$ = 36.826, p = .000006). Figure 4G shows that the magnitude of this radial difference in 12-Hz phase between moments in-time versus out-of-time was positively correlated with the benefit in accuracy for in-time compared with out-of-time targets on separate trials (circular-linear $r(22)$ = 0.578, $\chi^2(2)$ = 7.355, p = .025).

Phase-locking to Entrainers Is Modulated by Spatial Attention

Figure 5A shows the difference in PLI between the electrode ipsilateral to the cued direction of attention and the electrode contralateral to the cued direction, in electrodes P3 and P4, for target-present trials. If alpha lateralization influences this entrained activity, there should be

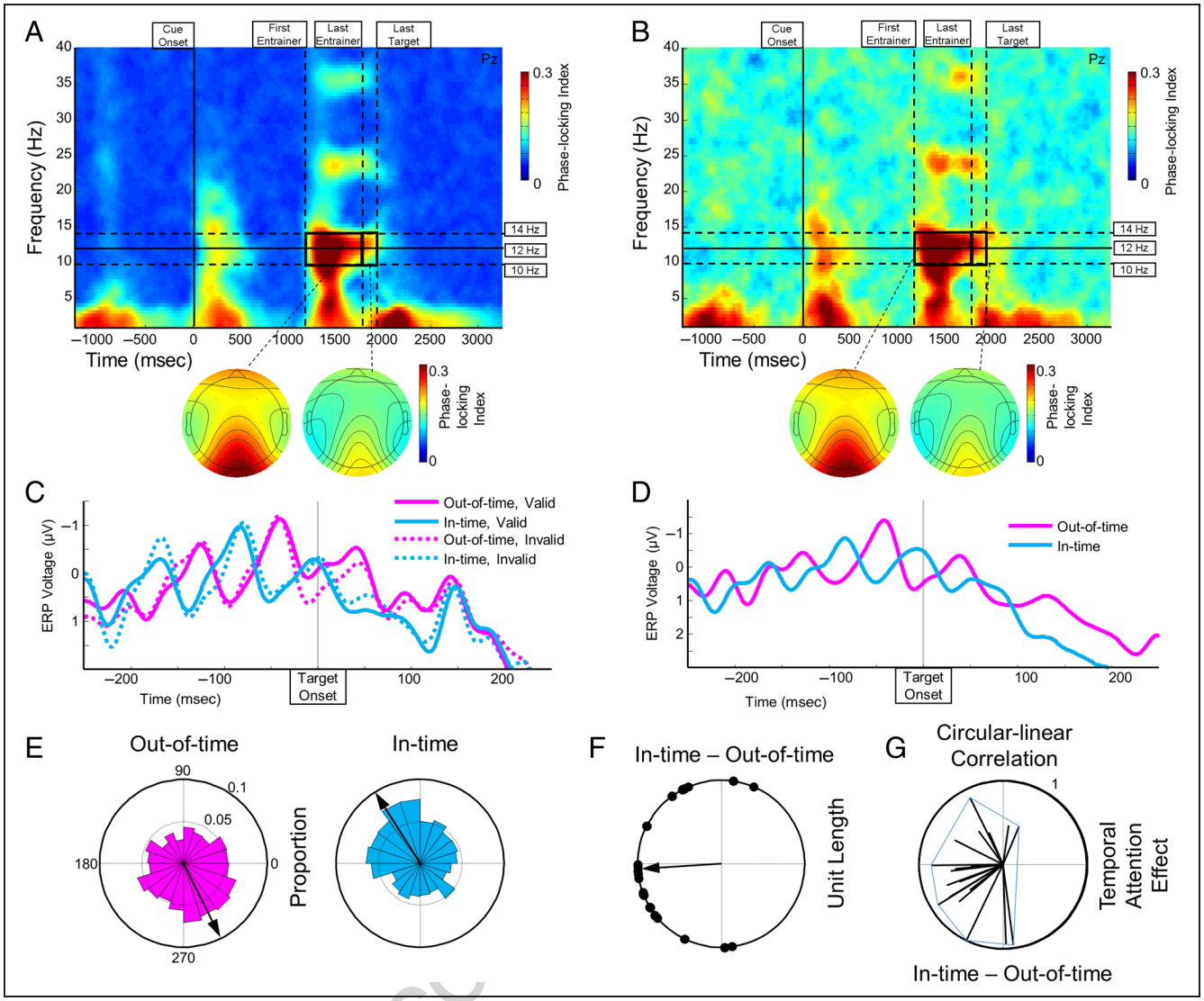

Figure 4. Temporal rhythms phase-locking alpha oscillations and influence performance. (A) A time–frequency representation of the PLI over the target-present trial from a single central electrode (Pz). Evident are broadband increases in PLI evoked by the important stimuli, along with a lasting increase in the phase locking at the entrainer frequency of 12 Hz, as well as two harmonics at 24 and 36 Hz. Scalp maps computed by averaging between 10 and 14 Hz during both an early (entrainment) and late (target) time period show that the PLI is maximal over visual cortex. Importantly, the phase-locking extends in time after the entrainers into the target period. (B) Shows the same analysis as in A for the 20% of trials where no target or mask were presented. (C) Shows the broadband ERPs time-locked to the moment that targets appeared on target-present trials. Evident is a 180° difference in the phase of oscillatory alpha activity time-locked to the entrainers that differs in phase between in-time (blue) and out-of-time (pink) target onset times. Solid and dashed lines represent separate groups of trials where targets were validly or invalidly cued by the spatially attention cue. (D) Shows the same data as in C but for target-absent trials. Note that spatially valid and invalid trials cannot be shown for target-absent trials. (E) Shows the resulting 12-Hz instantaneous phase at what would have been target onset in the 20% of trials when no target or mask were shown to avoid the influence of evoked target activity. A circular histogram shows the proportion of trials (pooled across all participants with no phase re-alignment) in each of 20 phase bins at the moments in-time (blue) and out-of-time (magenta) with the preceding rhythmic entrainment, showing opposite phase preferences for targets in-time versus out-of-time with the preceding rhythms. Arrows represent the average at unit length pooled over all trials for all participants, with around 180° difference between in-time and out-of-time moments. (F) Shows complementary information, indicating for each participant (dots) the radial difference between the circular mean across trials in-time versus out-of-time with the preceding rhythm. The arrow represents, at unit length, the grand average of these differences in phase. (G) Shows a visualization of the circular-linear correlation between the differences in average phase shown in E and the difference in behavioral accuracy between trials in-time versus out-of-time, computed on an independent set of trials. The angle represents the difference in alpha phase for a participant, and vector length indicates their temporal attention effect, rescaled to be positive between 0 and 1 for plotting. Longer lines closer to 180° indicate that participants with more 12-Hz phase locking had larger improvements in accuracy for targets in-time versus out-of-time. The blue line shows the convex hull of these vectors highlighting the clustering of longer lines on the left of the plot.

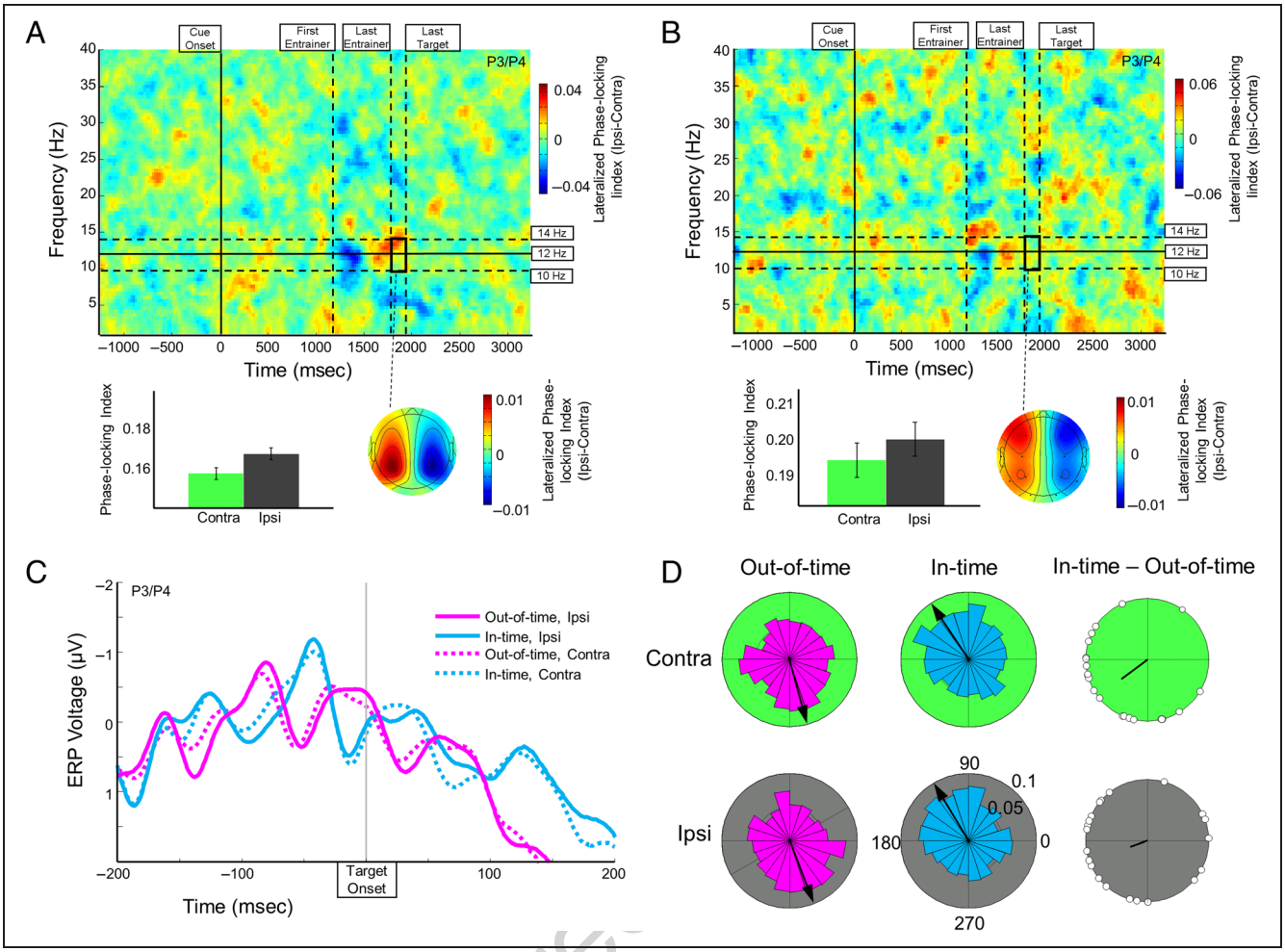

Figure 5. Markers of spatial and temporal attention in the brain interact. (A) Shows for target-present trials the difference in PLI subtracting electrodes contralateral from those ipsilateral to the direction of attention. This PLI is modulated by spatial attention in two periods: an early classic finding of increased phase locking contralateral to the rhythmic flashing during the entrainment period, followed by increased phase locking over posterior visual areas ipsilateral (black) compared with contralateral (green) from the direction of spatial attention during the target period. That is, the hemisphere with more lateralized alpha due to spatial attention shows more phase locking to rhythmic sequences. (B) The same test is shown for target-absent trials and showed an effect in the same direction that did not reach significance. (C) Shows the broadband ERPs time-locked to the moment that targets appeared on target-absent trials from lateral electrodes P3 and P4, separated by whether they were ipsilateral versus contralateral to the direction of attention. Evident is a 180° difference in the phase of oscillatory alpha activity time-locked to the entrainers that differs in phase between in-time (blue) and out-of-time (pink) target onset times. Here slightly larger phase locking is evident at electrode locations ipsilateral (solid) versus contralateral (dashed) to the direction of attention. (D) Shows the resulting 12-Hz instantaneous phase at what would have been target onset in the 20% of trials when no target or mask were shown to avoid the influence of evoked target activity, this time for lateral electrodes P3 and P4 sorted based into electrodes ipsilateral (gray back) versus contralateral (green back) to the direction of attention. Circular histograms show the proportion of trials (pooled across all participants with no phase re-alignment) in each of 20 phase bins at the moments in-time (blue) and out-of-time (magenta) with the preceding rhythmic entrainment, showing divergent phase preferences for targets in-time versus out-of-time with the preceding rhythms at both the ipsilateral and contralateral electrodes. Arrows represent the average at unit length pooled over all trials for all participants. On the right compass plots indicate for each participant (dots) the radial difference between the circular mean across trials in-time versus out-of-time with the preceding rhythm, for both ipsilateral and contralateral electrodes. The arrow represents the grand average direction and length of these differences in phase, showing consistent differences in phase between in-time and out-of-time target onsets periods at both the ipsilateral and contralateral electrodes.

phase-locking differences ipsilateral versus contralateral to the direction of attention, and this is observed to be centered on the entrainment frequency of 12 Hz and strongest in the target period. The bar graph indicates the average PLI in the target period window, showing a trend toward increased phase-locking at electrodes ipsilateral to the direction of attention (M = 0.1637, SD = 0.079) relative to contralateral (M = 0.1539, SD = 0.073; $t(21)$ = 1.6925, directional p = .0527). A scalp topography plot computed by averaging over the frequencies of 10–14 Hz during the late target window shows that the strongest lateralized difference is found over parietal electrodes. This increase reflects an interaction between spatial attention and entrainment, such that the alpha oscillations are more effectively entrained in the hemisphere representing the unattended locations,

where alpha oscillations are larger, mirroring the interaction between spatial and temporal attention. The same test on target-absent trials showed similar effects, but which were somewhat earlier, were more anterior, and did not reach significance at the same P3/P4 electrodes ($t(21) = 0.617$, *ns*), although there were only a small number of trials for some subjects. Lastly, we tested whether the difference in PLI on target-present trials would correlate with the behavioral interaction between spatial attention and temporal attention. Contrary to our prediction, these effects showed no correlation across subjects ($r = -.001$, $t(20) = 0.0067$, *ns*), although our relatively small number of subjects might preclude us from finding reliable across-subject correlations between these measures.

Lateralized Single-trial Phase at Target Onset Not Modulated by Spatial Attention

Figure 5C plots the peristimulus time of the broadband ERP locked to target onset for both out-of-time and in-time targets, now separately for electrodes ipsilateral (solid) versus contralateral (dashed) to the direction of attention. This plot again shows the 180° difference in the phase of dominant alpha oscillations at the time of target onset for targets in-time versus out-of-time with the preceding rhythmic entrainment. Figure 5C also indicates that this effect may be slightly enhanced at electrodes ipsilateral to the direction of attention, where alpha power is larger because of spatial attention modulations.

To test the interaction between spatial attention and single-trial phase position differences due to temporal attention, we next compared the phase of the entrained 12-Hz oscillation at target onset between targets in-time versus out-of-time with the preceding entrainers, but for electrodes P3 and P4, separated by when they were ipsilateral versus contralateral to the direction of the cue, and using only the trials in which no target was present to avoid the influence of evoked activity. Figure 5D shows histograms of these single-trial phases pooled over all trials and participants, revealing nonuniform distributions in 12-Hz phase at target onset. There was a large difference in phase at the onset of targets in-time versus out-of-time with the entrainers for electrodes both ipsilateral to the direction of attention (in-time pooled $M = 122.412°$, out-of-time $M = 292.194°$), as well as contralateral to the direction of attention (in-time pooled $M = 121.703°$, out-of-time $M = 286.455°$). To further examine whether or not this difference in phase was increased for electrodes ipsilateral to the direction of attention like the phase locking, we computed for each participant the circular mean over trials of the 12-Hz phase at target onset and compared these values for trials in-time versus out-of-time with entrainers and at ipsilateral and contralateral electrodes.

Figure 5D on the right shows for each participant the radial difference in grand mean phase between in-time and out-of-time targets for electrodes ipsilateral and contralateral to the direction of attention. The relative sign is kept intact to allow the values to range around the full circle. At electrodes ipsilateral to the direction of attention there was a reliable difference between targets in-time (grand $M = 123.170°$) and out-of-time with the entrainers (grand $M = 296.722°$; $M_{diff} = 201.278°$; Hotelling's bivariate $F(1, 20) = 40.1149$, $p < .001$). For the contralateral electrodes, there is also a large difference in phase between in-time targets (grand $M = 122.019°$) and out-of-time targets (grand $M = 292.484°$; $M_{diff} = 216.963°$; Hotelling's bivariate $F(1, 20) = 33.4151$, $p < .001$). Divergent from the PLI analysis, this difference was not reliably different at electrodes contralateral versus ipsilateral to the direction of attention ($M_{diff} = 357.264°$; Hotelling's bivariate $F(1, 20) = 0.1816$, *ns*), showing that the impact of spatial attention on target processing is not due to phase difference at target onset tested here but rather due to the inhibitory influence of that phase and the consistency over trials, as determined by lateralized power and phase locking.

DISCUSSION

A novel interaction was found between top–down visuospatial attention and bottom–up temporal entrainment to rhythmic stimuli. Metacontrast masked visual targets validly cued in space were better discriminated (Boyer & Ro, 2007). Alpha power was lateralized with spatial attention during the target period, with increased alpha ipsilateral versus contralateral to the cue direction (Rihs, Michel, & Thut, 2007; Kelly et al., 2006; Thut et al., 2006). There was a trend toward more lateralized alpha predicting the effect of spatial validity, supporting findings that spatial attention modulates inhibitory alpha oscillations to bias visual activity and behavior (Jensen et al., 2014; Mathewson et al., 2011; Jensen & Mazaheri, 2010; Klimesch et al., 2007).

Bottom–up temporal expectancy also influenced visual discrimination: targets presented in-time with preceding rhythmic stimuli were more effectively processed (Bauer, Jaeger, Thorne, Bendixen, & Debener, in press; Hickok et al., in press; Lawrance et al., 2014; Rohenkohl et al., 2012; Mathewson et al., 2010; Jones et al., 2002). Alpha phase was entrained by external visual rhythms (Spaak et al., 2014; de Graaf et al., 2013; Mathewson et al., 2012), with the phase of entrained oscillatory activity cyclically modulating visual discrimination as do endogenous oscillations (Busch et al., 2009; Mathewson et al., 2009) and as has also been shown in other frequency bands and modalities (ten Oever et al., 2015; Henry et al., 2014; Cravo, Rohenkohl, Wyart, & Nobre, 2013; Henry & Obleser, 2012; Stefanics et al., 2010). Larger alpha phase differences between targets in-time versus out-of-time predicted performance improvements for targets in-time with the entrainers (Mathewson et al., 2012). Temporal rhythms therefore align to the phase of

ongoing oscillations, serving as a mechanism for bottom–up temporal attention (Schroeder & Lakatos, 2009). It should be noted that some of these studies (Hickok et al., in press; Spaak et al., 2014) find better target performance out-of-time versus in-time with preceding entrainment. These differences may be due to the faster frequencies used in our current study as well as differences in stimulus properties, both possibilities that are currently being tested in our lab.

We have proposed that alpha oscillations represent a pulsed inhibition, controlled by top–down, goal-directed frontal regions (Mathewson et al., 2009, 2011, 2014), exerting inhibitory influence (Romei, Brodbeck, et al., 2008; Romei, Rihs, et al., 2008; Ergenoglu et al., 2004) via rhythmic periods of inhibitory neural silencing associated with certain phases of the alpha cycle (Mathewson et al., 2009). This theory accounts for bidirectional modulations in alpha power with attention (Rihs et al., 2007; Kelly et al., 2006; Thut et al., 2006) and behavior fluctuating with the phase of alpha oscillations (Cravo et al., 2015; Hanslmayr et al., 2013; Drews & VanRullen, 2011; Dugué et al., 2011; Hamm et al., 2010; Busch et al., 2009; Mathewson et al., 2009). The theory importantly predicts that phase effects on performance should be largest during high alpha power (Mathewson et al., 2011).

Here we show a novel interaction between spatial attention, lateralized alpha power, and subsequent rhythmic entrainment of these lateralized oscillations. The benefit for targets in-time with preceding rhythms was larger when presented to a brain area with larger alpha power. This finding reveals that the cyclical modulation of alpha phase on visual discrimination is largest during high alpha power (Mathewson et al., 2009). This is likely due to a stronger inhibitory influence, as well as larger portions of the oscillation phase being inhibitory (Jensen et al., 2014; Mathewson et al., 2011; Jensen & Mazaheri, 2010; Mazaheri & Jensen, 2008). Rhythmic entrainment interacted with lateralized alpha, such that the hemisphere with larger alpha power was better entrained. This suggests that induced temporal attention is most beneficial outside the focus of spatial attention. Interestingly, the attentional interaction in behavioral performance does not seem to be related to any differences in single trial phase separation (Figure 5D). This is understandable within our framework. A different phase distribution ipsilateral to the cue would have suggested that targets were being presented more precisely at a particular phase of the alpha cycle across trials and so were more likely to be inhibited. The observed equal phase differences as a function of attention, even with modulations in power and phase locking, suggests that targets were presented to the same phases, but the increased power and increased phase locking ipsilateral to attention-led targets that were presented to a given phase on the unattended side to be perceived differently than when they were presented at the same phase on the attended side. This may be due to increased period in an inhibitory phase (Mathewson et al., 2011) or more consistent phases over trials at unattended locations.

It is possible that the increase of phase locking ipsilateral to the cue is simply due to the increase in power, given that the estimate of phase is noisier when power is low. Previous research (Bonnefond & Jensen, 2012) has ruled out this possibility by showing independent effects of power and phase-locking in their data. In our data, however, it is the lateralization of alpha power before the entrainment period that facilitates entrainment, and so the effects are not expected to be entirely independent. However, if the increase in phase locking was entirely mediated by power, then we should expect to see a strong correlation in the ipsilateral minus contralateral difference between power and PLI, which is not observed (later period $r = -.09$, $t(20) = 0.408$, *ns*), suggesting that the ipsilateral increase in PLI is due to facilitated entrainment of endogenous rhythms and not due to a decrease in noise.

Spatial- and feature-based attention boosts steady-state activity induced by rhythmic stimuli (Gray et al., 2015; Kim, Grabowecky, Paller, & Suzuki, 2011; Kim, Grabowecky, Paller, Muthu, & Suzuki, 2007; Müller et al., 1998; Morgan, Hansen, & Hillyard, 1996). Attention to a sensory modality boosts low-frequency entrainment to rhythmic stimuli, improving performance for targets in-time with the rhythm (Besle et al., 2011; Gomez-Ramirez et al., 2011; Lakatos, Karmos, Mehta, Ulbert, & Schroeder, 2008), even with cross-modal targets (Escoffier, Herrmann, & Schirmer, 2015; ten Oever, Schroeder, Poeppel, van Atteveldt, & Zion-Golumbic, 2014). The steady-state effects of bottom–up rhythmic entrainers are larger when stimuli are spatially attended. The opposite effect of attention on neural entrainment observed here supports the idea that the same endogenous alpha oscillations that are lateralized by attention are also entrained by the rhythmic stimuli, because our observed effects were larger where and when alpha power was maximal. However, topographic maps of raw alpha power during the postcue interval (data not shown) show differences in topography between raw alpha and entrained alpha power. Future work should test for similarities and differences between endogenous oscillatory activity and that induced by rhythmic stimuli (see Keitel, Quigley, & Ruhnau, 2014).

Two recent studies have failed to find evidence that attention toward a sensory modality interacts with rhythmic entrainment. At slower timescales (<2 Hz), Jones (2014) manipulated spatial and temporal expectancies both between and across modalities. Participants reacted more quickly to targets appearing at attended locations and at times cued by the rhythmic stimuli. The entrainers were presented at fixation, not in the focus of attention as they are here. Additionally, Pomper, Keil, Foxe, and Senkowski (in press) had participants attend to one modality for either slow rhythmic or nonrhythmic stimuli. Target detection was faster in the attended modality, and for rhythmic stimulation, but with no interaction.

These results differ from the current finding in that the frequencies used do not correspond to the alpha oscillations lateralized by spatial attention and the entrainers are presented as distractors.

Alpha power also biases brain activity and behavior for longer-scale expectancies (>1 sec) using top–down temporal attention (Coull & Nobre, 1998), with decreased alpha power occurring during expected periods of target presentation (van Diepen et al., 2015; Rohenkohl & Nobre, 2011; Min et al., 2008). Our results confirm this finding, with increased power leading up to the period during which targets were expected to occur (with 166 msec uncertainty). Recently, van Diepen and colleagues (2015) failed to show evidence for top–down modulation of alpha phase over long periods (>1 sec) to expected target onset times. Modulations in power, not phase, were associated with longer-scale top–down influences of attention to upcoming moments. Rohenkohl, Gould, Pessoa, and Nobre (2014) showed that cues indicating both the spatial location and the upcoming timing of a relevant stimulus interact additively: Knowing when targets will occur only improves performance at spatially attended locations. This interaction between top–down spatial and top–down temporal attention is in the opposite direction as observed here between top–down spatial and bottom–up induced temporal expectancies. One explanation is that in this prior study the same mechanisms would be used to bias brain activity both spatially and temporally (alpha power); these effects evidently interact additively. However, Samaha and colleagues (2015), in a within-modality comparison of temporally predictive versus nonpredictive cues, found locking of preferred alpha phase around expected moments of target onset, but found no concurrent modulation in power.

Breska and Deouell (2014) found that bottom–up temporal expectations entrained by rhythmic stimuli occur even when targets are expected to occur at another time. Bottom–up entrainment by rhythmic sensory stimuli is automatic, occurring irrespective of top–down temporal expectations. These temporal expectancy effects for rhythms at unpredicted times were possibly observed because of increased alpha power during these inhibited time periods. Further research should test for interactions between top–down temporal attention and bottom–up temporal expectancies via alpha power and phase.

Finally, the periodic nature of perception as a function of the phase of ongoing alpha oscillations has been proposed to represent moments of discretized perceptual activity (Mathewson et al., 2011; VanRullen, Busch, Drewes, & Dubois, 2011; VanRullen & Koch, 2003). Indeed, rhythmic oscillations in perceptual performance even follow nonrhythmic events like sounds, attention cues, and TMS pulses (Landau & Fries, 2012; Romei, Gross, & Thut, 2012; VanRullen & Macdonald, 2012; Dehaene, 1993). Here we show new evidence that rhythmic stimuli in the world align perceptual frames to expected moments in time. It has been proposed that consciousness is not punctate or discrete but flows in a so-called stream of consciousness (Hickok et al., in press; Mathewson et al., 2012; James, 1890). Here we show that the stream may actually be coming through in waves, especially for stimuli outside our current focus of attention.

UNCITED REFERENCES

Doherty, Rao, Mesulam, & Nobre, 2005
Jaegle & Ro, 2014

Acknowledgments

This work was supported by a Natural Science and Engineering Research Council of Canada (NSERC) discovery grant (No. 04792) to Kyle E. Mathewson. The authors would like to thank Tyler Harrison for assistance with data collection. We also thank Claire Scavuzzo, Jeremy Caplan, and four anonymous reviewers for comments.

Reprint requests should be sent to Kyle E. Mathewson, P-217 Biological Sciences Building, Edmonton, Alberta, Canada, T6G 2E9, or via e-mail: kyle.mathewson@ualberta.ca.

REFERENCES

Barry, R. J., Rushby, J. A., Johnstone, S. J., Clarke, A. R., Croft, R. J., & Lawrence, C. A. (2004). Event-related potentials in the auditory oddball as a function of EEG alpha phase at stimulus onset. *Clinical Neurophysiology, 115,* 2593–2601.

Bauer, A. K. R., Jaeger, M., Thorne, J. D., Bendixen, A., & Debener, S. (in press). The auditory dynamic attending theory revisited: A closer look at the pitch comparison task. *Brain Research*.

Berens, P. (2009). CircStat: A MATLAB toolbox for circular statistics. *Journal of Statistical Software, 31,* 1–21.

Besle, J., Schevon, C. A., Mehta, A. D., Lakatos, P., Goodman, R. R., McKhann, G. M., et al. (2011). Tuning of the human neocortex to the temporal dynamics of attended events. *Journal of Neuroscience, 31,* 3176–3185.

Bonnefond, M., & Jensen, O. (2012). Alpha oscillations serve to protect working memory maintenance against anticipated distracters. *Current Biology, 22,* 1969–1974.

Bonnefond, M., & Jensen, O. (2015). Gamma activity coupled to alpha phase as a mechanism for top–down controlled gating. *PLoS One, 10,* e0128667.

Boyer, J., & Ro, T. (2007). Attention attenuates metacontrast masking. *Cognition, 104,* 135–149.

Breska, A., & Deouell, L. Y. (2014). Automatic bias of temporal expectations following temporally regular input independently of high-level temporal expectation. *Journal of Cognitive Neuroscience, 26,* 1555–1571.

Buhusi, C. V., & Meck, W. H. (2005). What makes us tick? Functional and neural mechanisms of interval timing. *Nature Reviews Neuroscience, 6,* 755–765.

Busch, N. A., Dubois, J., & VanRullen, R. (2009). The phase of ongoing EEG oscillations predicts visual perception. *Journal of Neuroscience, 29,* 7869–7876.

Busch, N. A., & VanRullen, R. (2010). Spontaneous EEG oscillations reveal periodic sampling of visual attention. *Proceedings of the National Academy of Sciences, U.S.A., 107,* 16048–16053.

Callaway, E., & Yeager, C. L. (1960). Relationship between reaction time and electroencephalographic alpha phase. *Science, 132,* 1765–1766.

Coull, J. T., & Nobre, A. C. (1998). Where and when to pay attention: The neural systems for directing attention to spatial locations and to time intervals as revealed by both PET and fMRI. *Journal of Neuroscience, 18,* 7426–7435.

Cravo, A. M., Rohenkohl, G., Wyart, V., & Nobre, A. C. (2013). Temporal expectation enhances contrast sensitivity by phase entrainment of low-frequency oscillations in visual cortex. *Journal of Neuroscience, 33,* 4002–4010.

de Graaf, T. A., Gross, J., Paterson, G., Rusch, T., Sack, A. T., & Thut, G. (2013). Alpha-band rhythms in visual task performance: Phase-locking by rhythmic sensory stimulation. *PLoS One, 8,* e60035.

Dehaene, S. (1993). Temporal oscillations in human perception. *Psychological Science, 4,* 264–270.

Delorme, A., & Makeig, S. (2004). EEGLAB: An open source toolbox for analysis of single-trial EEG dynamics. *Journal of Neuroscience Methods, 134,* 9–21.

Doherty, J. R., Rao, A., Mesulam, M. M., & Nobre, A. C. (2005). Synergistic effect of combined temporal and spatial expectations on visual attention. *Journal of Neuroscience, 25,* 8259–8266.

Drews, J., & VanRullen, R. (2011). This is the rhythm of your eyes: The phase of ongoing electroencephalogram oscillations modulates saccadic reaction time. *Journal of Neuroscience, 31,* 4698–4708.

Dugué, L., Marque, P., & VanRullen, R. (2011). The phase of ongoing oscillations mediates the causal relation between brain excitation and visual perception. *Journal of Neuroscience, 31,* 11889–11893.

Ergenoglu, T., Demiralp, T., Bayraktaroglu, Z., Ergen, M., Beydagi, H., & Uresin, Y. (2004). Alpha rhythm of the EEG modulates visual detection performance in humans. *Cognitive Brain Research, 20,* 376–383.

Escoffier, N., Herrmann, C. S., & Schirmer, A. (2015). Auditory rhythms entrain visual processes in the human brain: Evidence from evoked oscillations and event-related potentials. *Neuroimage, 111,* 267–276.

Fisher, N. (1993). *Statistical analysis of circular data*. Cambridge, UK: Cambridge UP.

Gomez-Ramirez, M., Kelly, S. P., Molholm, S., Sehatpour, P., Schwartz, T. H., & Foxe, J. J. (2011). Oscillatory sensory selection mechanisms during intersensory attention to rhythmic auditory and visual inputs: A human electrocorticographic investigation. *Journal of Neuroscience, 31,* 18556–18567.

Gratton, G., Coles, M. G. H., & Donchin, E. (1983). A new method for off-line removal of ocular artifact. *Electroencephalography and Clinical Neurophysiology, 55,* 468–484.

Gray, M. J., Frey, H. P., Wilson, T. J., & Foxe, J. J. (2015). Oscillatory recruitment of bilateral visual cortex during spatial attention to competing rhythmic inputs. *Journal of Neuroscience, 35,* 5489–5503.

Haegens, S., Cousijn, H., Wallis, G., Harrison, P. J., & Nobre, A. C. (2014). Inter- and intra-individual variability in alpha peak frequency. *Neuroimage, 92,* 46–55.

Haegens, S., Nácher, V., Luna, R., Romo, R., & Jensen, O. (2011). Alpha oscillations in the monkey sensorimotor network influence discrimination performance by rhythmical inhibition of neuronal spiking. *Proceedings of the National Academy of Sciences, U.S.A., 108,* 19377–19382.

Hamm, J. P., Dyckman, K. A., Ethridge, L. E., McDowell, J. E., & Clementz, B. A. (2010). Preparatory activations across a distributed cortical network determine production of express saccades in humans. *Journal of Neuroscience, 30,* 7350–7357.

Hanslmayr, S., Volberg, G., Wimber, M., Dalal, S. S., & Greenlee, M. W. (2013). Prestimulus oscillatory phase at 7 Hz gates cortical information flow and visual perception. *Current Biology, 23,* 2273–2278.

Henry, M. J., Herrmann, B., & Obleser, J. (2014). Entrained neural oscillations in multiple frequency bands comodulate behavior. *Proceedings of the National Academy of Sciences, U.S.A., 111,* 14935–14940.

Henry, M. J., & Obleser, J. (2012). Frequency modulation entrains slow neural oscillations and optimizes human listening behavior. *Proceedings of the National Academy of Sciences, U.S.A., 109,* 20095–20100.

Herrmann, C. S. (2001). Human EEG responses to 1–100 Hz flicker: Resonance phenomena in visual cortex and their potential correlation to cognitive phenomena. *Experimental Brain Research, 137,* 346–353.

Hickok, G., Farahbod, H., & Saberi, K. (in press). The rhythm of perception entrainment to acoustic rhythms induces subsequent perceptual oscillation. *Psychological Science*.

Jacobs, J., Kahana, M. J., Ekstrom, A. D., & Fried, I. (2007). Brain oscillations control timing of single-neuron activity in humans. *Journal of Neuroscience, 27,* 3839–3844.

Jaegle, A., & Ro, T. (2014). Direct control of visual perception with phase-specific modulation of posterior parietal cortex. *Journal of Cognitive Neuroscience, 26,* 422–432.

James, W. (1890). *The principles of psychology (Vol. 1)*. Holt.

Jansen, B. H., & Brandt, M. E. (1991). The effect of the phase of prestimulus alpha activity on the averaged visual evoked response. *Electromyography and Clinical Neurophysiology, 80,* 241–250.

Jensen, O., Gips, B., Bergmann, T. O., & Bonnefond, M. (2014). Temporal coding organized by coupled alpha and gamma oscillations prioritize visual processing. *Trends in Neurosciences, 37,* 357–369.

Jensen, O., & Mazaheri, A. (2010). Shaping functional architecture by oscillatory alpha activity: Gating by inhibition. *Frontiers in Human Neuroscience, 4*.

Jones, A. (2014). Independent effects of bottom–up temporal expectancy and top–down spatial attention. An audiovisual study using rhythmic cueing. *Frontiers in Integrative Neuroscience, 8*.

Jones, M. R., Moynihan, H., MacKenzie, N., & Puente, J. (2002). Temporal aspects of stimulus-driven attending in dynamic arrays. *Psychological Science, 13,* 313–319.

Keitel, C., Quigley, C., & Ruhnau, P. (2014). Stimulus-driven brain oscillations in the alpha range: Entrainment of intrinsic rhythms or frequency-following response? *Journal of Neuroscience, 34,* 10137–10140.

Kelly, S. P., Lalor, E. C., Reilly, R. B., & Foxe, J. J. (2006). Increases in alpha oscillatory power reflect an active retinotopic mechanism for distracter suppression during sustained visuospatial attention. *Journal of Neurophysiology, 95,* 3844–3851.

Kim, Y. J., Grabowecky, M., Paller, K. A., Muthu, K., & Suzuki, S. (2007). Attention induces synchronization-based multiplicative response gain in steady-state visual evoked potentials. *Nature Neuroscience, 10,* 117–125.

Kim, Y. J., Grabowecky, M., Paller, K. A., & Suzuki, S. (2011). Differential roles of frequency-following and frequency-doubling visual responses revealed by evoked neural harmonics. *Journal of Cognitive Neuroscience, 23,* 1875–1886.

Klimesch, W., Sauseng, P., & Hanslmayr, S. (2007). EEG alpha oscillations: The inhibition-timing hypothesis. *Brain Research Reviews, 53,* 63–88.

Lakatos, P., Karmos, G., Mehta, A. D., Ulbert, I., & Schroeder, C. E. (2008). Entrainment of neuronal oscillations as a mechanism of attentional selection. *Science, 320,* 110–113.

Landau, A. N., & Fries, P. (2012). Attention samples stimuli rhythmically. *Current Biology, 22,* 1000–1004.

Large, E. W., & Jones, M. R. (1999). The dynamics of attending: How we track time-varying events. *Psychological Review, 106,* 119–159.

Lawrance, E. L., Harper, N. S., Cooke, J. E., & Schnupp, J. W. (2014). Temporal predictability enhances auditory detection. *Journal of the Acoustical Society of America, 135,* EL357–EL363.

Loftus, G. R., & Masson, M. E. (1994). Using confidence intervals in within-subject designs. *Psychonomic Bulletin & Review, 1,* 476–490.

Lőrincz, M. L., Kékesi, K. A., Juhász, G., Crunelli, V., & Hughes, S. W. (2009). Temporal framing of thalamic relay-mode firing by phasic inhibition during the alpha rhythm. *Neuron, 63,* 683–696.

Mathewson, K. E., Fabiani, M., Gratton, G., Beck, D. M., & Lleras, A. (2010). Rescuing stimuli from invisibility: Inducing a momentary release from visual masking with pre-target entrainment. *Cognition, 115,* 186–191.

Mathewson, K. E., Gratton, G., Fabiani, M., Beck, D. M., & Ro, T. (2009). To see or not to see: Prestimulus alpha phase predicts visual awareness. *Journal of Neuroscience, 29,* 2725–2732.

Mathewson, K. E., Lleras, A., Beck, D. M., Fabiani, M., Ro, T., & Gratton, G. (2011). Pulsed out of awareness: EEG alpha oscillations represent a pulsed-inhibition of ongoing cortical processing. *Frontiers in Psychology, 2*.

Mathewson, K. E., Prudhomme, C., Fabiani, M., Beck, D. M., Lleras, A., & Gratton, G. (2012). Making waves in the stream of consciousness: Entraining oscillations in EEG alpha and fluctuations in visual awareness with rhythmic visual stimulation. *Journal of Cognitive Neuroscience, 24,* 2321–2333.

Mazaheri, A., & Jensen, O. (2008). Asymmetric amplitude modulations of brain oscillations generate slow evoked responses. *Journal of Neuroscience, 28,* 7781–7787.

Min, B. K., Park, J. Y., Kim, E. J., Kim, J. I., Kim, J. J., & Park, H. J. (2008). Prestimulus EEG alpha activity reflects temporal expectancy. *Neuroscience Letters, 438,* 270–274.

Morgan, S. T., Hansen, J. C., & Hillyard, S. A. (1996). Selective attention to stimulus location modulates the steady-state visual evoked potential. *Proceedings of the National Academy of Sciences, U.S.A., 93,* 4770–4774.

Müller, M. M., Teder-Sälejärvi, W., & Hillyard, S. A. (1998). The time course of cortical facilitation during cued shifts of spatial attention. *Nature Neuroscience, 1,* 631–634.

Pastor, M. A., Artieda, J., Arbizu, J., Valencia, M., & Masdeu, J. C. (2003). Human cerebral activation during steady-state visual-evoked responses. *Journal of Neuroscience, 23,* 11621–11627.

Pomper, U., Keil, J., Foxe, J. J., & Senkowski, D. (in press). Intersensory selective attention and temporal orienting operate in parallel and are instantiated in spatially distinct sensory and motor cortices. *Human Brain Mapping*.

Posner, M. I. (1980). Orienting of attention. *Quarterly Journal of Experimental Psychology, 32,* 3–25.

Rihs, T. A., Michel, C. M., & Thut, G. (2007). Mechanisms of selective inhibition in visual spatial attention are indexed by α band EEG synchronization. *European Journal of Neuroscience, 25,* 603–610.

Rohenkohl, G., Cravo, A. M., Wyart, V., & Nobre, A. C. (2012). Temporal expectation improves the quality of sensory information. *Journal of Neuroscience, 32,* 8424–8428.

Rohenkohl, G., Gould, I. C., Pessoa, J., & Nobre, A. C. (2014). Combining spatial and temporal expectations to improve visual perception. *Journal of Vision, 14,* 8.

Rohenkohl, G., & Nobre, A. C. (2011). Alpha oscillations related to anticipatory attention follow temporal expectations. *Journal of Neuroscience, 31,* 14076–14084.

Romei, V., Brodbeck, V., Michel, C., Amedi, A., Pascual-Leone, A., & Thut, G. (2008). Spontaneous fluctuations in posterior alpha-band EEG activity reflect variability in excitability of human visual areas. *Cerebral Cortex, 18,* 2010–2018.

Romei, V., Gross, J., & Thut, G. (2012). Sounds reset rhythms of visual cortex and corresponding human visual perception. *Current Biology, 22,* 807–813.

Romei, V., Rihs, T., Brodbeck, V., & Thut, G. (2008). Resting electroencephalogram alpha-power over posterior sites indexes baseline visual cortex excitability. *NeuroReport, 19,* 203–208.

Samaha, J., Bauer, P., Cimaroli, S., & Postle, B. R. (2015). Top–down control of the phase of alpha-band oscillations as a mechanism for temporal prediction. *Proceedings of the National Academy of Sciences, U.S.A., 112,* 8439–8444.

Schroeder, C. E., & Lakatos, P. (2009). Low-frequency neuronal oscillations as instruments of sensory selection. *Trends in Neurosciences, 32,* 9–18.

Spaak, E., Bonnefond, M., Maier, A., Leopold, D. A., & Jensen, O. (2012). Layer-specific entrainment of gamma-band neural activity by the alpha rhythm in monkey visual cortex. *Current Biology, 22,* 2313–2318.

Spaak, E., de Lange, F. P., & Jensen, O. (2014). Local entrainment of alpha oscillations by visual stimuli causes cyclic modulation of perception. *Journal of Neuroscience, 34,* 3536–3544.

Stefanics, G., Hangya, B., Hernádi, I., Winkler, I., Lakatos, P., & Ulbert, I. (2010). Phase entrainment of human delta oscillations can mediate the effects of expectation on reaction speed. *Journal of Neuroscience, 30,* 13578–13585.

ten Oever, S., Schroeder, C. E., Poeppel, D., van Atteveldt, N., & Zion-Golumbic, E. (2014). Rhythmicity and cross-modal temporal cues facilitate detection. *Neuropsychologia, 63,* 43–50.

ten Oever, S., van Atteveldt, N., & Sack, A. T. (2015). Increased stimulus expectancy triggers low-frequency phase reset during restricted vigilance. *Journal of Cognitive Neuroscience, 27,* 1811–1822.

Thut, G., Nietzel, A., Brandt, S., & Pascual-Leone, A. (2006). Alpha-band electroencephalographic (EEG) activity over occipital cortex indexes visuospatial attention bias and predicts visual target detection. *Journal of Neuroscience, 26,* 9494–9502.

van Diepen, R. M., Cohen, M. X., Denys, D., & Mazaheri, A. (2015). Attention and temporal expectations modulate power, not phase, of ongoing alpha oscillations. *Journal of Cognitive Neuroscience, 27,* 1573–1586.

VanRullen, R., Busch, N. A., Drewes, J., & Dubois, J. (2011). Ongoing EEG phase as a trial-by-trial predictor of perceptual and attentional variability. *Frontiers in Psychology, 2*.

VanRullen, R., & Koch, C. (2003). Is perception discrete or continuous? *Trends in Cognitive Sciences, 7,* 207–213.

Varela, F. J., Toro, A., John, E. R., & Schwartz, E. L. (1981). Perceptual framing and cortical alpha rhythm. *Neuropsychologia, 19,* 675–686.

Watson, A. B., & Pelli, D. G. (1983). QUEST: A Bayesian adaptive psychometric method. *Perception & Psychophysics, 33,* 113–120.

Zar, J. H. (1999). *Biostatistical analysis* (4th ed.). Prentice-Hall Inc.

AUTHOR QUERIES

AUTHOR PLEASE ANSWER ALL QUERIES

During the preparation of your manuscript, the questions listed below arose. Kindly supply the necessary information.

1. Sheeringa et al., 2011, was not cited in the reference list. Please check.
2. Cravo et al., 2015, was not cited in the reference list. Please check.
3. Cravo et al., 2012, was not cited in the reference list. Please check.
4. Brainard, 1997, was not cited in the reference list. Please check.
5. Please provide manufacturer location (EasyCap).
6. Please verify manufacturer location (Electro-Medical Instruments).
7. Behrens, 2009, was not cited in the reference list. Please check.
8. Mathewson et al., 2014, was not cited in the reference list. Please check.
9. VanRullen & Macdonald, 2012, was not cited in the reference list. Please check.
10. Please insert citations of these references in the body: Doherty, Rao, Mesulam, & Nobre, 2005; Jaegle & Ro, 2014.
11. Please update publication status and details of Bauer et al., in press.
12. Please update publication status and details of Hickok et al., in press.
13. Please provide publisher location of James, 1890.
14. Please provide page numbers of Jensen & Mazaheri, 2010.
15. Please provide page numbers of Jones, 2014.
16. Please provide page numbers of Mathewson et al., 2011.
17. Please update publication status and details of Pomper et al., in press.
18. Please provide page numbers of VanRullen et al., 2011.
19. Please provide publisher location of Zar, 1999.

END OF ALL QUERIES